

## Recrystallisation Characteristics of a Cu-Bearing HSLA Steel Assessed Through High Temperature Compressive Deformation

Atul Kumar<sup>#,\*</sup>, T.V.V.S. Vara Prasad<sup>§</sup>, V.V. Karthik<sup>!</sup>, Kumkum Banerjee<sup>!</sup>,  
K. Gopinath<sup>#</sup> and R. Balamuralikrishnan<sup>#</sup>

<sup>#</sup>DRDO-Defence Metallurgical Research Laboratory, Kanchanbagh, Hyderabad - 500 058, India

<sup>§</sup>National Institute of Technology, Warangal - 506 004, India

<sup>!</sup>National Institute of Technology Karnataka, Surathkal - 575 025, India

\*E-mail: atul.dmrl@gov.in

### ABSTRACT

Dynamic (DRX) operative during deformation and static recrystallisation (SRX) operative after deformation are considered responsible for the changes in microstructure and texture of deformed materials. Especially in the case of advanced steels that are required in the form of plates of various thicknesses, hot rolling is the main manufacturing process during which the steel undergoes DRX under the rolls and SRX between rolling passes/strands. Knowledge on DRX and SRX characteristics of such steels is crucial for optimisation of hot rolling parameters, achieving the desired microstructure and consequently the targeted mechanical properties. In this study, certain key aspects of both dynamic (DRX) and static recrystallisation (SRX) behaviour of a Cu-bearing HSLA steel, which was developed at DMRL, have been explored through high temperature deformation studies using Gleeble thermo-mechanical simulator. Through uniaxial compression testing in the austenitic regime, domains of continuous and discontinuous DRX prevalent in the steel were identified and critical parameters for initiation of dynamic recrystallisation viz., critical strain ( $\epsilon_c$ ), critical stress ( $\sigma_c$ ), peak stress ( $\sigma_p$ ) and peak strain ( $\epsilon_p$ ) were determined as a function of temperature and strain rate. SRX characteristics were assessed through uniaxial double hit compression tests with fixed strain rate and strain per hit but at different temperatures and with different imposed intermediate static recrystallisation (ISRT) times. From the fractional softening data, parameters such as time for 50 % recrystallisation,  $t_{0.5}$ , temperature for 50 % recrystallisation,  $T_{0.5}$ , and activation energy, QSRX have been estimated. Although the steel exhibited good plastic deformation characteristics, the results suggest that the role of copper in retarding recrystallisation is significant.

**Keywords:** Dynamic recrystallisation; Static recrystallization; Uniaxial compression test; Gleeble

### 1. INTRODUCTION

High Strength Low Alloy (HSLA) steels are an important category of steels used in industrial and structural applications especially in automotive, oil and gas extraction, agricultural machinery, defence and offshore applications<sup>1</sup> in view of their attractive combination of tensile strength, toughness, formability and weldability, which are key for use of materials in such structural applications<sup>2-3</sup>. The microstructure responsible for attainment of the required combination of properties in this class of steels is strongly dependent on the processing route and process parameters. Hot rolling of steel is one of the most widely used hot working processes during which strain, strain rate, temperature and interpass time are required to be optimised to achieve the desired properties in flat products. Recrystallisation is an important metallurgical phenomenon that takes place not only during deformation in the presence of temperature and applied stress (termed dynamic recrystallisation, DRX) but also during any hold

times at high temperature and cooling down from deformation temperatures when applied stress is absent (termed static recrystallisation, SRX and Meta-Dynamic Recrystallisation, MDRX). As recrystallisation involves nucleation and growth of fresh strain-free grains from a deformed material, it alters the grain structure that in turn, plays a crucial role in dictating the mechanical properties of materials. Thus, a thorough understanding of recrystallisation is fundamental in deciding the hot rolling schedule of any given steel.

This work is aimed at characterising DRX and SRX behaviour of a copper-bearing HSLA steel being explored by Defence Metallurgical Research Laboratory (DMRL) for potential naval structural applications. These applications require steels in the form of plates of various thicknesses. Such plates are manufactured through hot rolling during which the steel undergoes both DRX and SRX. To understand DRX behaviour, it is necessary to determine the critical conditions (strain and stress) required for initiation of DRX as a function of deformation temperature and strain rate. Similarly, to study the SRX behaviour, recrystallisation characteristics need to be understood as a function of recrystallisation time and

temperature. Towards this, single hit and double hit uniaxial compression tests have been employed to assess DRX and SRX characteristics, respectively using the Gleeble thermo-mechanical simulator. The experimental results are analysed in detail and discussed in light with the published literature on other steels to gain an understanding on the recrystallisation behaviour of the steel under study. The critical parameters experimentally determined through this work are also crucial inputs for development of models for capturing DRX and SRX behaviour leading to the prediction of microstructure and properties in turn.

**2. EXPERIMENTAL WORK**

The nominal composition of the steel is given in Table 1. On the basis of dilatometry carried out earlier, the upper ( $A_{c3}$ ) and lower ( $A_{c1}$ ) critical temperatures for this steel were  $765 \pm 7^\circ\text{C}$  and  $698 \pm 13^\circ\text{C}$  respectively<sup>4</sup>. Therefore, test temperatures for characterising both DRX and SRX behaviour were selected such that deformation takes place in the fully austenitic regime, i.e., above  $775^\circ\text{C}$ .

**Table 1. Nominal composition of the steel studied (wt. %)**

C	Si	Mn	Ni+Cu	Cr+Mo
0.09	0.2-0.3	1.2	4-6	0.4-1.5

Both DRX and SRX studies were carried out on cylindrical compression test specimens with dimensions of 10 mm in diameter by 15 mm in height, machined out from a hot-rolled plate produced on industrial scale. The specimens were extracted in such a way that specimen axis remains parallel to the rolling direction i.e. the specimens were compressed along the rolling direction during the uniaxial compression tests. Test specimens used for carrying out both DRX and SRX studies were subjected to identical heating schedules before imparting deformation in compression. The specimens were first heated to a temperature of  $1200^\circ\text{C}$ , high in the fully austenitic regime, at a heating rate of  $5^\circ\text{C}/\text{sec}$  to dissolve all the precipitate phases present in the material and then cooled to selected deformation

temperatures at a cooling rate of  $2^\circ\text{C}/\text{sec}$ . The specimen was given a dwell time of 60 sec at the deformation temperature so as to ensure uniformity in temperature throughout the specimen.

For carrying out DRX studies, at the selected deformation temperatures of 800, 850, 900, 950, 1000 and  $1100^\circ\text{C}$ , the specimens were compressed to a true strain of 1.0 at different strain rates ranging from  $10^{-3} \text{ s}^{-1}$  to  $10^{-1} \text{ s}^{-1}$  and the stress-strain response was captured. For carrying out SRX studies, double hit compression tests (DHCT) were carried out at selected deformation temperatures of 800, 850, 875, 900, 950,  $1000^\circ\text{C}$  and  $1050^\circ\text{C}$ . DHCT involves two successive compressive deformation steps (also called as “hits”) on a single specimen with the hits separated by an imposed time interval<sup>5-6</sup>.

The first compressive deformation in a DHCT basically imparts the desired strain at a desired strain rate and temperature, during which the stress-strain response of the material is captured. This is followed by a time interval during which the specimen temperature is controlled to maintain the deformation temperature without any stress imposed on it. The material undergoes SRX during this time interval. Immediately after the imposed time interval, a second hit is imparted to the specimen to the same strain level at the same strain rate and temperature as that of the first hit. The stress-strain response of the material captured during the second hit is a reflection of the extent of static recrystallisation undergone by the material during the imposed hold, i.e., intermediate static recrystallisation time (ISRT). Using the stress-strain data pertaining to the first and second deformation, an estimate of the fractional softening due to SRX is deduced as described in 5.2 ‘Fractional Softening’. In this study, the first and second deformation in compression were carried out by applying a true strain of 0.2 at a true strain rate of 10/s. ISRTs imposed were 10, 100 and 500 sec. Thus, the effects of both important variables, i.e. SRX time and temperatures on the SRX behaviour could be studied systematically. All the deformed specimens were air cooled to room temperature after deformation. A schematic of these experiments carried out for characterising DRX and SRX behaviour is shown in Fig. 1.

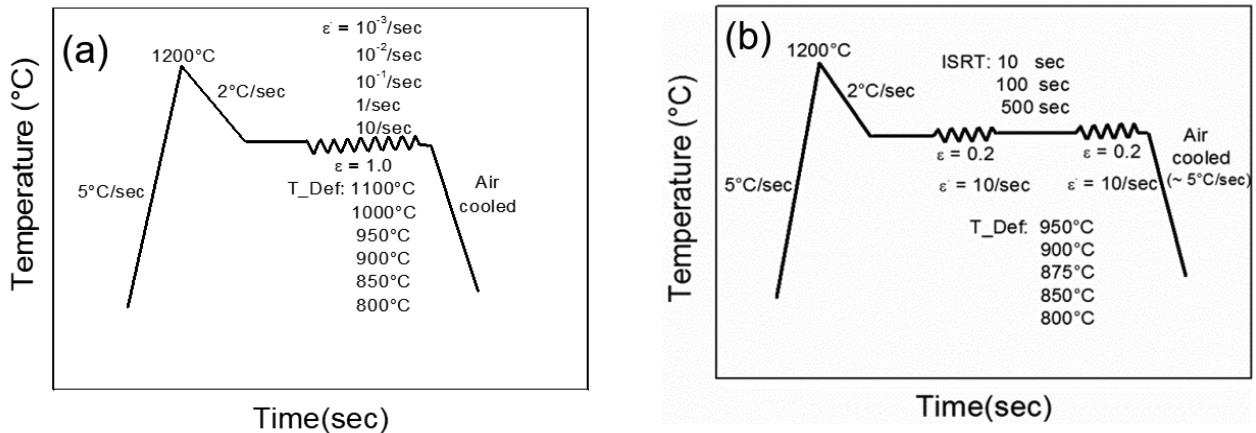


**Figure 1. Schematic representation of thermo-mechanical cycle adopted for studying: (a) DRX behaviour in single stage uniaxial compression and (b) SRX behaviour in double hit compression<sup>7</sup>.**

All the above compression tests were carried out using Hydrowedge module in a Gleeble 3800 system in vacuum ( $\sim 1.0 \times 10^{-6}$  torr), which adopts Joule heating method to heat the specimens. K-type thermocouples (of diameter 0.02 mm) were spot welded to the surface of the specimen at the centre of its height. These thermocouple were used for both purposes, as feedback control of the specimen temperature as well as for specimen temperature measurements.

### 3. RESULTS AND DISCUSSION

Physical examination of all the specimens subjected to DRX and SRX studies revealed that the specimen surfaces were free from any cracks. Dimensional inspection of deformed specimens confirmed that the intended strain levels could be achieved in all the tests. Details of the analyses carried out on the true stress-strain data captured from the compression tests to understand the DRX and SRX behaviour of the material under study are presented in the sections below.

### 4. DRX BEHAVIOUR

#### 4.1 Flow Curves

Representative true stress-true strain curves for the material compressed at various temperatures with different strain rates are shown in Fig. 2. Figure 2(a) shows the stress-strain plots at different temperatures at a fixed true strain rate of 0.001 / sec, and Fig. 2(b) shows the same at different strain rates but at a fixed temperature of 1100 °C. All the flow curves are very similar in the beginning of deformation where the flow stresses exhibit a linear elastic regime followed by onset of plastic deformation. In the early stages of plastic deformation, all the curves exhibit an increase in flow stress with increase in strain. However, at higher strain levels the behaviour of flow curves can be categorised into three types: (a) Type I, where the flow stresses rise marginally with increase in strain and then tend to saturate at a constant stress level after the onset of plastic flow. This behaviour is observed in 16 of the 30 temperature / strain rate combination studied and is observed at high strain rates and low temperatures, (b) Type II, where the flow curves first reach a peak stress level and then exhibit a drop in stress levels

with increase in strain which then tends to gradually stabilise at higher strains. This single-peak behaviour is observed in 11 out of the 30 temperature/strain rate combination explored in this study and is observed at intermediate temperature/strain rate combinations, (c) Type III, which is similar to Type II and exhibits a drop in stress level initially from a peak stress level, but with increase in strain levels tends to exhibit hardening again followed by softening in a cyclic fashion. Presence of multiple peaks in such cases is illustrated in magnified plots in Fig. 3. This behaviour, seen at high temperature and low strain rates, is observed only in 3 of the 30 conditions studied.

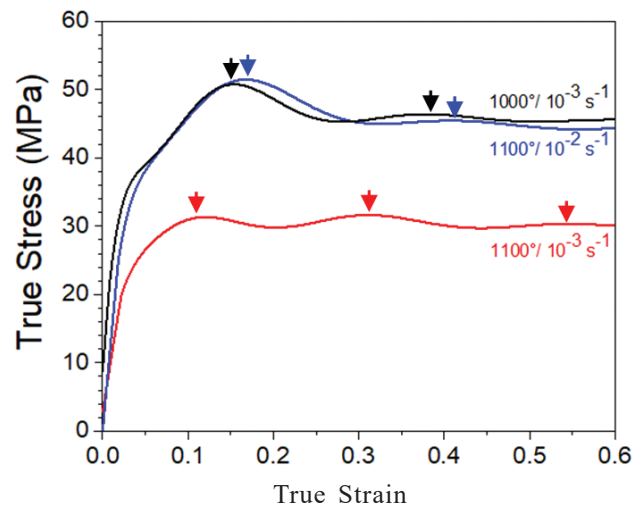


Figure 3. Presence of multiple peaks observed in true  $\sigma$ - $\epsilon$  curves.

A few of the flow curves classified as Type I, especially at the higher strain rates, show increasing stress levels when strain levels exceed 0.7. This is typical when friction between the specimen and anvils increase<sup>8</sup> and additional load is required to be applied to achieve deformation at specified rates. Although graphite was used as lubricant during the experiments, it is effective in reducing friction only at lower strain levels and hence, frictional effects couldn't be avoided at higher strain levels. It is usual to correct the flow curves

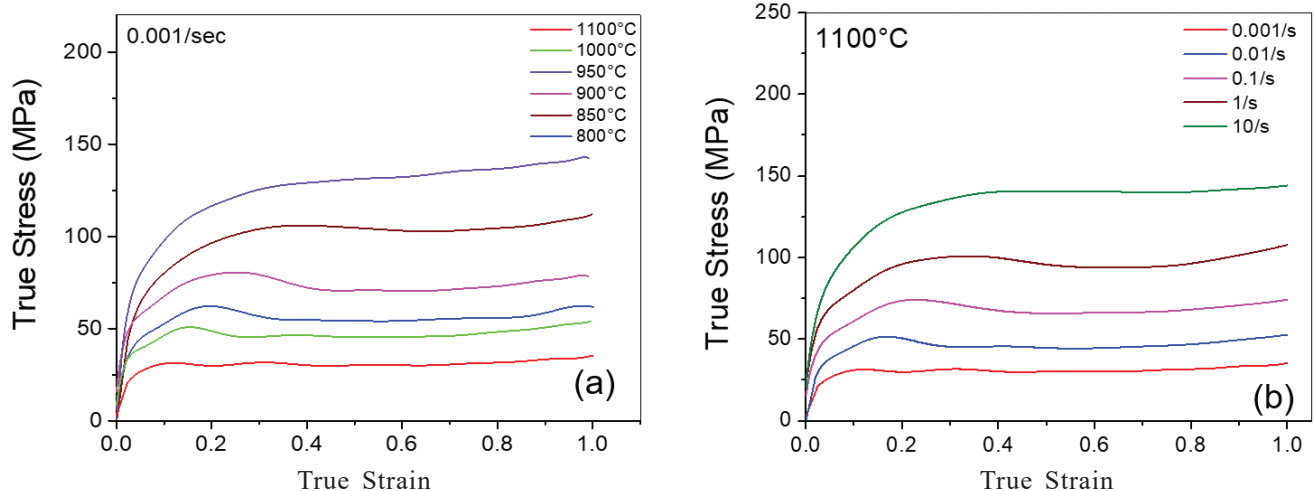


Figure 2. Representative true  $\sigma$ - $\epsilon$  curves: (a) at different temperatures at a fixed strain rate 0.001/sec and (b) at different strain rates at a fixed deformation temperature of 1100 °C.

for friction effects to make use of the stress values especially at higher strain levels<sup>8-9</sup>. However, as would be discussed in subsequent sections, as most of the attention in this work is for assessment of DRX behaviour focussed on the portion of the flow curve below strain levels of 0.5, no stress correction was adopted as part of this study.

**4.2 DRX Characteristics**

The nature of the flow curves suggest that hardening and counteracting softening mechanisms operate during plastic straining. In the rising segments of the flow curves, hardening mechanisms dominate over the softening mechanisms. At strain levels beyond the peak stress when the flow stresses drop, softening mechanisms dominate over the hardening mechanisms. It is known that dynamic recovery is a softening mechanism that prevails at all strain levels during plastic deformation<sup>10</sup>. Similarly, dynamic recrystallisation, which initiates after accumulation of sufficient levels plastic strain and at sufficiently high temperatures, is another important softening mechanism<sup>10</sup>.

Type II flow curves with a single peak in true stress-strain curves are clearly an indication of continuous dynamic recrystallisation (cDRX) in which the peak stress/strain

corresponds to the point beyond which softening due to recrystallisation dominates over work hardening<sup>11</sup>. Type III flow curves exhibiting multiple peaks are suggestive of discontinuous Dynamic Recrystallisation (dDRX) associated with repetitive hardening followed by softening<sup>11</sup>.

From published studies, it is clear that, even in materials and conditions that exhibit Type I flow curves, DRX could prevail even if it does not show up as single or multiple peaks. Presence of an inflection point in  $d\sigma/d\varepsilon$  vs  $\sigma$  curves<sup>12-13</sup> is considered an indication of initiation of DRX in materials, rather than an inference from the shape of flow curves. Irrespective of the type of flow curve, the strain corresponding to the point of inflection, termed critical strain,  $\varepsilon_c$  is considered to represent the deformation necessary to initiate DRX. The critical strain is known to be a function of chemical composition, grain size and deformation conditions (viz., temperature and strain rate)<sup>14</sup>. It was initially understood that DRX is initiated during deformation when a critical dislocation density is attained<sup>15</sup>, on the basis of evolution of densities of mobile dislocations and stored dislocations in cell walls and cell interiors. However, it was later brought out that the point of inflection on the  $d\sigma/d\varepsilon$  vs  $\sigma$  curves corresponds to the point of conversion of rigid cell walls to mobile sub boundaries<sup>16</sup>. In order to determine

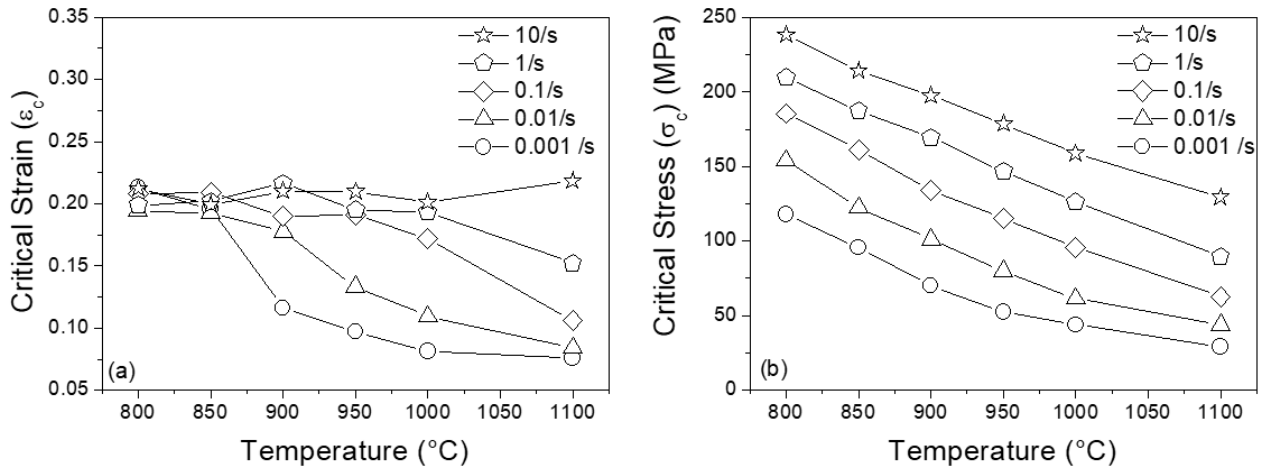


Figure 4. Variation of (a)  $\varepsilon_c$  and (b)  $\sigma_c$  with temperature at different strain rates.

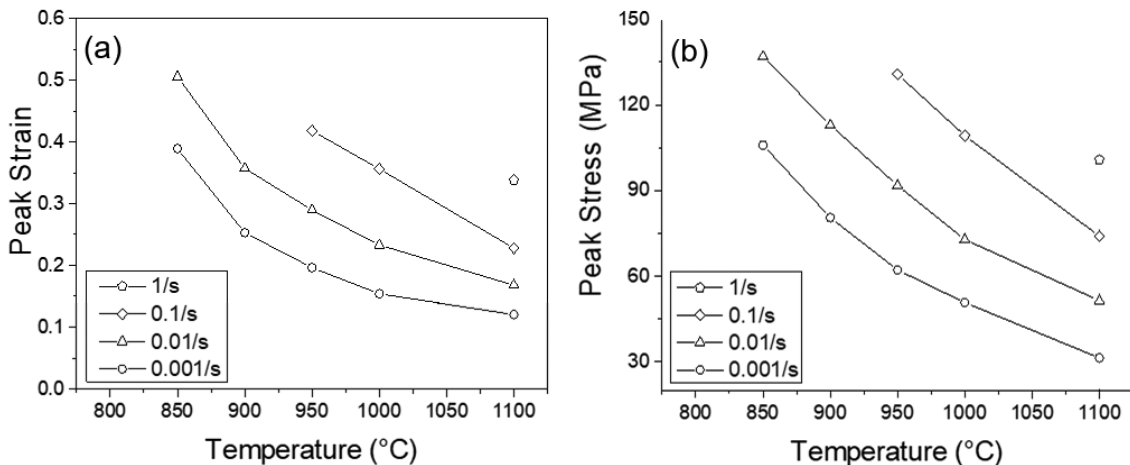


Figure 5. Variation of (a)  $\varepsilon_p$  and (b)  $\sigma_p$  with temperature at different strain rates.

$\epsilon_c$  from the experimentally captured flow curves, a double differentiation method, developed and adopted by Poliak, *et al.*<sup>12-13</sup>, was employed through a MATLAB program developed for this purpose. This involves determination of work hardening rate,  $\theta(=d\sigma/d\epsilon)$  as a function of stress. Subsequently, the critical stress,  $\sigma_c$  corresponding to the point of inflection on  $d\theta/d\sigma$  vs  $\sigma$  curves is identified precisely as the minima on the plot of  $d\theta/d\sigma$  vs  $\sigma$ . The strain corresponding to  $\sigma_c$  on the  $\sigma$ - $\epsilon$  plot is identified as  $\epsilon_c$ .

## 5. CRITICAL PARAMETERS IN DRX

Although initiation of DRX manifests in the second differential ( $d\theta/d\sigma$ ) based on which critical strain  $\epsilon_c$  is identified, it is explicitly manifested on flow curves only when a significant fraction recrystallises and the resulting softening dominates the concurrent hardening thereby reducing the flow stress levels beyond a peak stress level,  $\sigma_p$  and associated peak strain,  $\epsilon_p$ . Subsequently flow stresses reach a steady state after which the stresses remain constant with increasing strain levels. The steady state strain,  $\epsilon_{ss}$ , represents the strain level where the recrystallisation of initial material is complete<sup>17</sup>. Hence,  $\epsilon_c$ ,  $\sigma_c$ ,  $\epsilon_p$  and  $\sigma_p$  are considered key parameters of significance in characterising the DRX behaviour of materials.

The dependence of  $\epsilon_c$  and  $\sigma_c$  on deformation temperature and strain rate is shown in Fig. 4. It is observed (Fig. 4(a)) that, irrespective of the strain rate,  $\epsilon_c$  is nearly constant at about 0.2 for the lower temperatures of 800 and 850°C. Beyond 850°C,  $\epsilon_c$  reduces with increase in temperature at all strain rates. However, at the highest strain rate of 10 s<sup>-1</sup>,  $\epsilon_c$  tends to be a constant at about 0.2 irrespective of the temperature.

Similarity in evolution of substructure responsible for initiation of DRX at low temperatures and higher strain rates could be responsible for similarity in  $\epsilon_c$  levels under these conditions. As discussed earlier,  $\epsilon_c$  is indicative of the critical dislocation density required for initiation of DRX, which is strongly dependent on the imposed deformation conditions<sup>15</sup>. The observed trend of reduction in  $\epsilon_c$  with increase in temperature and decrease in strain rate is likely due to the achievement of the necessary critical dislocation density for initiation of DRX at lower strain levels because of the increased thermal assistance that is available at higher temperatures, and the ease

of diffusion assisted nucleation<sup>18</sup> that directly influences the recrystallisation.

Dynamic recrystallisation (DRX) is a diffusion controlled process. At high strain rates and for a given strain, not enough time is available for diffusion mechanisms to operate. Thus, the effect of temperature tends to diminish at higher strain rates, which manifests as almost constant critical strains for initiation of DRX for longer range of temperatures as seen in the case of 10 s<sup>-1</sup>. The independence of critical strain on temperature within the range of 800-1100°C at the highest strain rate studied of 10 s<sup>-1</sup> suggest predominant effect of strain rate over temperature unlike at other combinations of strain rate and temperature where both temperature and strain rates have significant contributions. Critical stress decreases with strain rate and temperature as depicted in Fig. 4(b). Figure 5 shows the trend exhibited by peak strain (Fig. 5(a)) and stress (Fig. 5(b)) with varying temperature and strain rates in cases where the flow curves exhibited clear peaks. It is reported that increasing strain rate and decreasing temperature slows down the process of nucleation and growth of DRX grains, which is a softening process<sup>19</sup>. As the peak strain / stress marks the point where softening effects dominate over hardening effects, reduced nucleation and growth with increasing strain rate increases peak stress and strain values.

Plot showing the relationship between  $\epsilon_c$  and  $\epsilon_p$  is shown in Fig. 6a. Data points pertaining to all temperatures and strain rates where a clear peak could be observed are included in the plot without differentiating between them on the basis of strain rates and temperatures. The plot reveals that a clear linear correlation ( $\epsilon_c = 0.39\epsilon_p + 0.02$ ; Adj. R<sup>2</sup> = 0.93) between  $\epsilon_c$  and  $\epsilon_p$  exists independent of temperature and strain rate. The average value of the ratio between  $\epsilon_c$  and  $\epsilon_p$  is observed to be 0.48. The value obtained is within the range reported (0.37 – 0.83) for many other steels viz., 0.37-0.39 for low and medium carbon vanadium micro alloyed steels<sup>20</sup>, 0.4 for X70 pipeline steel<sup>21</sup>, 0.47 for 17-4 PH stainless steel<sup>22</sup>, 0.48 for low carbon vanadium-nitrogen micro alloyed steel<sup>23</sup>, 0.73 for 304 stainless steel<sup>24</sup> and 0.7-0.83 in Nb and Nb-Ti micro alloyed steels<sup>25</sup>.

A similar plot of  $\sigma_c$  vs  $\sigma_p$  is shown in Fig. 6b. Similar to  $\epsilon_c$ , a linear correlation ( $\sigma_c = 0.91\sigma_p - 2.35$ ; Adj. R<sup>2</sup> = 0.99) could be observed between  $\sigma_c$  and  $\sigma_p$ , independent of temperature and

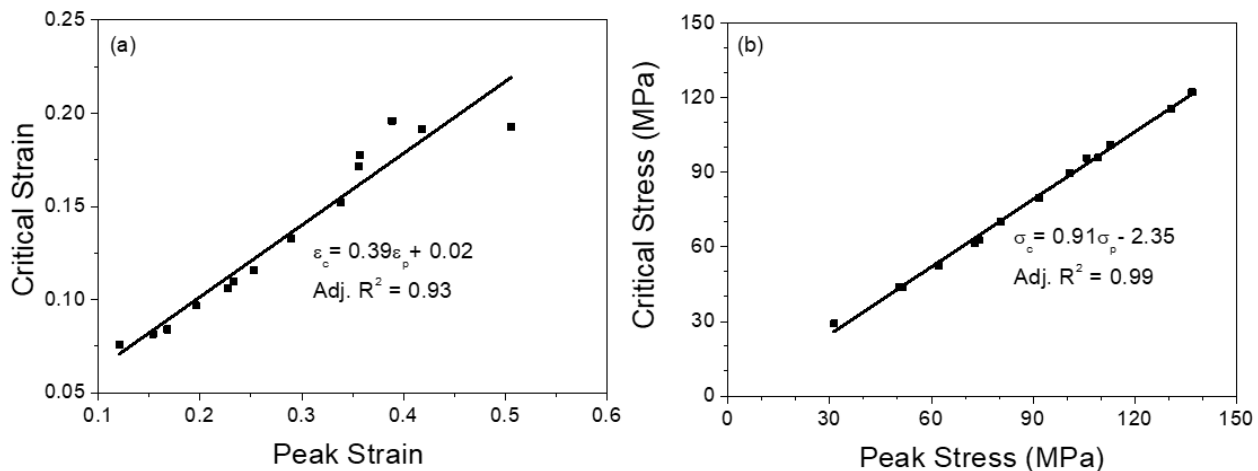


Figure 6. Relationship between (a) Critical strain ( $\epsilon_c$ ) and Peak strain ( $\epsilon_p$ ), (b) Critical stress ( $\sigma_c$ ) and Peak stress ( $\sigma_p$ )

strain rate. The average value of the ratio between  $\sigma_c$  and  $\sigma_p$  is observed to be 0.88. This is in line with values reported for other steels viz., 0.83 for low and medium carbon vanadium micro alloyed steels<sup>18</sup> and X70 pipeline steel<sup>21</sup>, 0.89 for 17-4 PH stainless steel<sup>22</sup>. The average value of ratio between  $\epsilon_c$  and  $\epsilon_p$ , and  $\sigma_c$  and  $\sigma_p$ , are parameters that shed light on the extent of work hardening the material undergoes before softening effects dominate. While lower ratio values suggest early initiation of DRX with respect to the peak strain / stress, higher ratio values suggests quicker progression of recrystallisation induced softening leading to dominance of softening over hardening. While peak stresses and strains are parameters which can be ascertained directly from the flow curves, determination of critical strains and critical stresses thereof involves detailed analyses of data and are therefore not easily readable from flow curves. However, with the knowledge of a linear dependence between critical and peak strains and the slope, which varies narrowly within a given class of steel, one can easily estimate roughly the level of strain that will trigger dynamic recrystallisation in any given steel.

**6. SRX BEHAVIOUR**

**6.1 Double Hit Compression Tests**

True stress-strain plots of the studied steel obtained by carrying out DHCTs carried out at different temperatures using an ISRT of 100 sec are shown in Fig. 7(a). The first set of 5 curves on the left represents the stress-strain curves pertaining to first deformation. The second set of 5 curves represents the stress-strain response from the second deformation imparted after imposition of specified ISRT, in this case, 100 sec. The temperature effect on the flow stress is evident in the systematic lowering of flow stress with increasing deformation temperature in both the deformation segments.

Figure 7(b) depicts the influence of ISRT on the stress-strain curves pertaining to second deformation at a fixed temperature, in this case, 950°C. Only one representative curve pertaining to first deformation is shown in Fig. 7(b) as they are similar for all the three tests. The effect of increasing ISRT that would result in increased SRX and attendant softening is evident in the systematic shifting of flow curves in the downward direction, as shown in Fig. 7(b). A very systematic

trends similar to that in Fig. 7(a) and Fig. 7(b) were observed at all other ISRTs and deformation temperatures, respectively.

**6.2 Fractional Softening**

Extent of SRX is estimated indirectly, direct being metallographically, from DHCT data through ‘Fractional Softening (FS)’, a parameter that quantifies net softening in the material. As the stacking fault energy of this class of steels is expected to be low<sup>26</sup>, it is considered that softening due to recovery is negligible and the net softening is fully attributable to recrystallisation. While multiple methods<sup>27</sup> are compared to estimate fractional softening, mean flow stress (MFS) method, which is popular, especially when effect of recovery is excluded<sup>28</sup>, has been adopted in this study.

The FS values computed from DHCT data are presented as a function of temperature in Fig. 8 for the three ISRTs studied. It is clear from Fig. 8 that, FS values varied between 0.21 and 0.99 for the range of deformation temperatures and ISRTs studied, though fractional softening can have any value between 0 and 1 (both inclusive). For a fixed temperature, fractional softening, that is an indicator of the extent of recrystallisation, increases with increase in ISRT. This is in line with the understanding that recrystallisation, being a diffusion controlled process and therefore dependent on temperature and time, would proceed

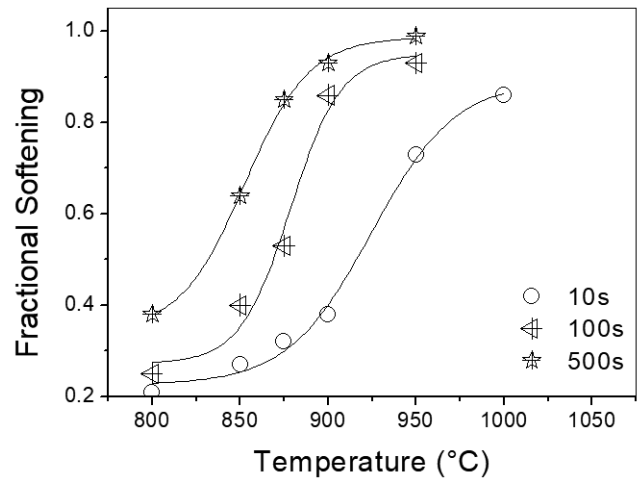


Figure 8. Change in fractional softening with temperature for different ISRTs<sup>7</sup>.

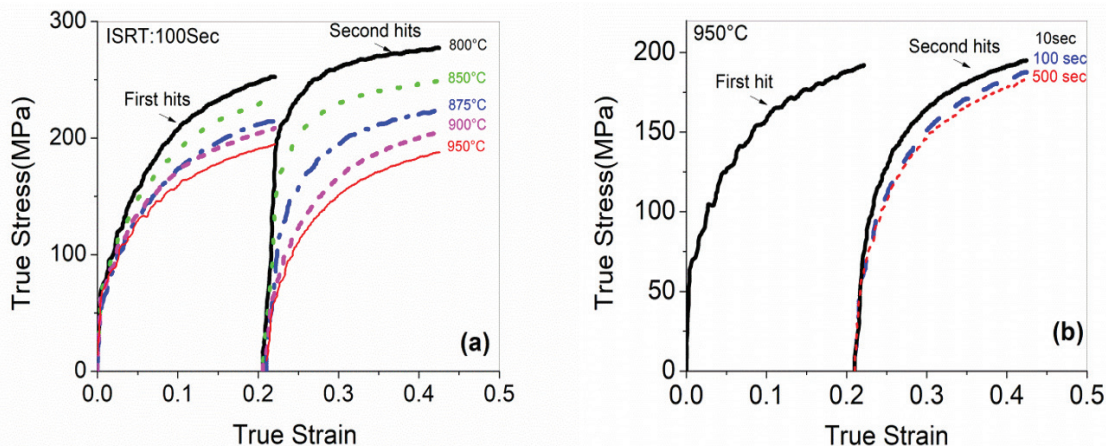


Figure 7. Typical true stress-strain curves obtained from DHCT of studied steel<sup>7</sup>: (a) for different temperatures at a fixed ISRT 100 sec (b) for different ISRTs at a fixed temperature 950 °C.

to higher completion levels for longer ISRTs at any given temperature. For ISRT of 100 and 500s, FS values show a trend to first increase and then saturate to values closer to 1.

**6.3 Characterisation of Static Recrystallisation (SRX) Behaviour**

Since static recrystallisation is a diffusion controlled process, its kinetics are described by a Johnson-Mehl-Avrami-Kolmogorov (JMAK) type equation given below<sup>29</sup>:

$$FS = 1 - \exp \left[ -0.693 \left( \frac{t}{t_{0.5}} \right)^n \right] \tag{1}$$

where, ' $t_{0.5}$ ' corresponds to the time for 50 % recrystallisation at a given temperature, FS is the fraction of the recrystallised volume in time, ' $t$ ' and ' $n$ ' is the Avrami exponent.  $n$  has been determined as slope of  $\ln \left( \ln \left( \frac{1}{1 - FS} \right) \right)$  and  $\ln(t)$

plots. Using the experimental data generated in this study, such straight line fits with  $R^2$  values exceeding 0.9 could be obtained using the data available at three ISRTs at five temperatures (plots not included here). The values of Avrami's exponent,  $n$  determined for the temperatures studied are given in Table 2. The value of Avrami's exponent ( $n$ ) is normally related to the phenomenon of nucleation and growth of recrystallised grains<sup>30</sup>. For isotropic growth over pre-existing nuclei at the start of recrystallisation, the value of  $n$  is expected to be 3. In addition, if new nuclei are created at a constant rate in the unrecrystallised material, the value of  $n$  is predicted to be 4.

When growth is in less than three dimensions and nucleation is heterogeneous, the values of  $n$  lower than 3 are predicted. However, especially in low carbon microalloyed steels and HSLA steels, low values of  $n$ -like 0.7<sup>31</sup>, 0.6<sup>32</sup> and 0.55<sup>33</sup> have also been reported. However, Avrami's exponent, by nature, is independent of temperature and hence no trend in its variation with temperature can be meaningful. That's why this is not plotted and presented as a table to convey the point that the obtained exponents vary only within a small range (0.17-0.45) indicating that the mechanism involved in recrystallisation is essentially the same across the temperature range studied.

**Table 2. Value of Avrami's exponent at different temperatures for SRX in the steel studied**

Temperature (°C)	Avrami's exponent, $n$
800	0.17
850	0.29
875	0.40
900	0.45
950	0.32

Since  $n$  corresponds to the rate of SRX with respect to time, it is evident that the rate of recrystallisation is relatively low in the steel studied in comparison with other classes of steels in general, exact reasons for which are not yet clear and it is to be explored in details in future work.

For the steel studied,  $t_{0.5}$ , i.e. the time for 50 % recrystallisation, which are determined as intercepts in the

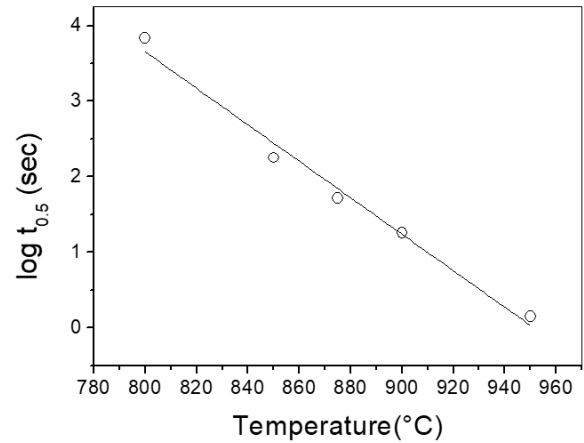


**Figure 9. Variation of time for 50 % static recrystallisation ( $t_{0.5}$ ) with temperature<sup>7</sup>.**

linear fits discussed above, exhibited a strong dependence on temperature which is a major driving force for SRX (Fig. 9). Time intervals between deformation stages in industrial hot working processes, during which SRX takes place, can be large (typical in plate rolling and forging) or small (typical of processes like strip rolling)<sup>34</sup>. From prior knowledge of  $t_{0.5}$ , time interval between hot working stages can be increased to increase volume recrystallised (in roughing operations) or decreased during finishing operations (as in TMP steels) to increase as-worked strength levels.

Using the values of  $n$  and  $t_{0.5}$ , plots of FS determined as per Eqn. 2 were constructed for different temperatures as a function of SRX time (shown as solid lines in Fig. 10). FS computed using MFS method for the ISRTs that could be imposed experimentally are also shown in the plot as symbols. Given the typical industrial interpass times, plots like in Fig. 10 can provide valuable inputs in selecting appropriate roughing hot rolling temperatures at which FS closer to 1 could be achieved. Similarly, for thermo-mechanically controlled finish rolling stages, appropriate low temperatures can be chosen for desired low SRX levels.

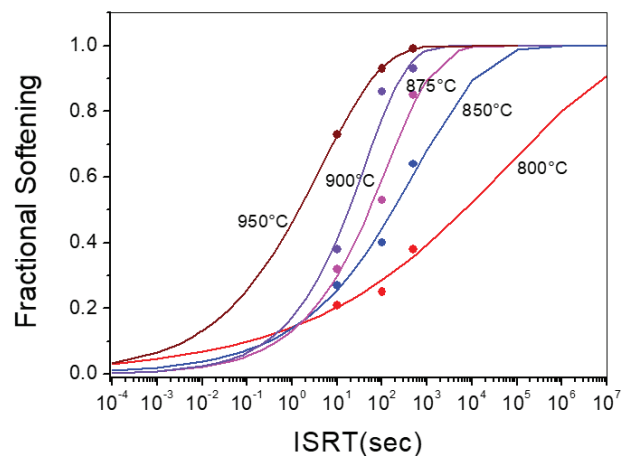


**Figure 10. Fractional softening (FS) versus Intermediate static recrystallisation times (ISRTs) at different temperatures<sup>7</sup>; symbols are the points determined from analysis of experimental data and the lines are the FS values computed from equation (1).**

#### 6.4 Temperature for 50 % Recrystallisation, $T_{0.5}$

From the plots in Fig. 8, another critical parameter, viz., temperature for 50 % SRX,  $T_{0.5}$  can be extracted for every ISRT as the temperature corresponding to FS of 0.5. This is in principle similar to the more popular non-recrystallisation temperature,  $T_{NR}$ , which signifies the temperature below which SRX no longer goes to completion in the given ISRT between the two successive deformations<sup>35</sup>. As  $T_{NR}$  is a practically and industrially significant parameter, it is generated specifically for a steel considering appropriate levels of strains, strain rates and interpass times typical of the rolling mill in which the steel is proposed to be rolled. It is also defined with respect to FS, typically 0.2<sup>36</sup>. As this study is generic and not specific to any such parameters, the term  $T_{NR}$  is not being used. It can be seen from Fig. 8 that  $T_{0.5}$  reduces with increasing ISRT. This is plotted separately in Fig. 11, which clearly shows the effect

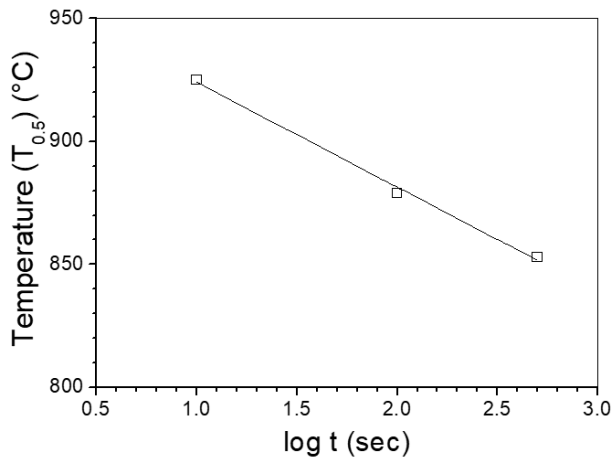


Figure 11. Variation of temperature for 50 % static recrystallisation,  $T_{0.5}$  with time (ISRT)<sup>7</sup>.

of ISRT on  $T_{0.5}$ . Though it is known that temperature for 50 % SRX and ISRT are inversely related, a linear relationship as depicted in Fig. 11 could be observed when ISRT is plotted on a logarithmic scale.

#### 6.5 Activation Energy for Static Recrystallisation

Progress of SRX at a given temperature is captured through the expression below<sup>37</sup>:

$$t_{0.5} = A_{SRX} \cdot \exp\left(\frac{Q_{SRX}}{RT}\right) \quad (2)$$

where,  $R = 8.314 \text{ J/(mol. K)}$ ,  $T$  is absolute temperature,  $Q_{SRX}$  is the activation energy for SRX, and  $A_{SRX}$  is the constant that depends on strain rate, strain and grain size. Activation energy for recrystallisation  $Q_{SRX}$  can be determined from the slope of the plot of  $1/T$  vs  $\ln t_{0.5}$  depicted in Fig. 12 for the steel studied. The activation energy for the studied steel is determined to be 608 kJ/mol as against values ranging from 160 – 780 kJ/mol<sup>38</sup> reported in literature depending on the composition of the steel. In general, alloying elements tend to increase activation energy for SRX. Solid solution-strengthening elements in austenite tend to retard recrystallisation through solute drag effects<sup>39</sup>. The motion of dislocations and grain boundaries, which are crucial for progression of static recrystallisation, are likely to be restricted due to enrichment of alloying elements at their

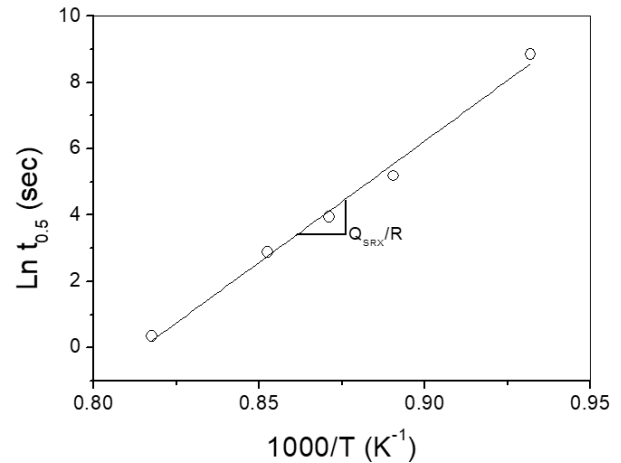


Figure 12. Variation of time for 50% static recrystallisation,  $t_{0.5}$  with temperature<sup>7</sup>.

sites. Considering that a Cu-Nb-B steel exhibited similar activation energy level (559 kJ/mol)<sup>40</sup>, the presence of copper could be one of the reasons for the relatively higher activation energy level exhibited by the steel studied.

#### 7. CONCLUSIONS

Recrystallisation characteristics of a Cu-Bearing HSLA steel studied through high temperature compressive deformation revealed the following:

- The systematic variation in temperature - strain rate combinations that lead to flow curves with no peaks, single peak (cDRX) and multiple peaks (dDRX) in the steel studied could be identified
- Critical strain,  $\epsilon_c$  and critical stress,  $\sigma_c$  for initiation of DRX in the material studied could be determined as a function of temperature and strain rate from the experiments. A linear correlation could be established between critical stress and peak stress as well as critical strain and peak strain
- Critical parameters that describe SRX viz., fractional softening, FS, time for 50 % recrystallisation,  $t_{0.5}$ , temperature for 50 % recrystallisation,  $T_{0.5}$ , Avrami exponent,  $n$  and activation energy,  $Q_{SRX}$  have been determined from DHCTs.

#### REFERENCES

1. Skobir, Danijela A. High Strength Low-Alloy (HSLA). *Materials and Technol.*, 2011, **45**, 295–301.
2. Rashid, M.S. High-Strength Low-Alloy Steels, *Science*, 1980, **208**, 862-869.  
doi: 10.1126/science.208.4446.862
3. Porter, L.F. & Repas, P.E. The evolution of HSLA steels. *J. Metals*, April 1982, 14-21.  
doi: 10.1007/BF03337994
4. Vara Prasad, T.V.V.V.S. Gleeble based studies on Thermo-mechanical processing of a Cu-Bearing HSLA naval steel, 2017, M.Tech. Thesis, National Institute of Technology, Warangal.
5. DeArdo, A.J. Niobium in modern steels. *Int. Materials Rev.* 2003, **48**, 371–402.  
doi:10.1179/095066003225008833

6. Palmiere, E.J.; Garcia, C.I. & DeArdo, A.J. The Influence of niobium supersaturation in austenite on the static recrystallization behavior of low carbon microalloyed steels, *Metall. Mater. Transact.*, 1996, **27**, 951–960.  
doi:10.1007/BF02649763
7. Kumar, A.; Vara Prasad, T.; Nazeer, M.; Gopinath, K. & Balamuralikrishnan, R. A study of recrystallization behaviour of two Ni-Cu-Containing high-strength steels with different Mn contents. *Mater. Perform. Charact.*, 2020, **9**, 89-100.  
doi: 10.1520/MPC20190034
8. Li, Y.P.; Ondodera, E.; Matsu, H. Oto & Chiba, A. Correcting the stress-strain curve in hot-compression process to high strain level. *Metall. Mater. Transact.*, 2009, **40A**, 982-990.  
doi:10.1007/s11661-009-9783-7
9. Ebrahimi, R. & Najafizadeh, A. A new method for evaluation of friction in bulk metal forming. *J. Mater. Process. Technol.*, 2004, **152**, 136–143.  
doi:10.1016/j.jmatprotec.2004.03.029
10. Ebrahimi, R. & Solhjoo, S. Characteristic points of stress-strain curve at high temperature. *Int. J. ISSI*, 2007, **4**, 24-27.
11. Sakai, T. & Jonas, J.J. Dynamic recrystallization: mechanical and microstructural considerations. *Acta Metall.*, 1984, **32**, 189-209.  
doi: 10.1016/0001-6160 (84)90049-X
12. Poliak, E.I. & Jonas, J.J. A one-parameter approach to determining the critical conditions for the initiation of dynamic recrystallization, *Acta Mater.* 1996, **44**, 127-136.  
doi: 10.1016/1359-6454 (95)00146-7
13. Poliak, E.I. & Jonas, J.J. Initiation of dynamic recrystallization in constant strain rate hot deformation. *ISIJ International*, 2003, **43**, 692-700.  
doi: 10.2355/isijinternational.43.684
14. Castro-Fernandez, F.R.; Sellars, C.M. & Whiteman, J.A. Changes of flow-stress and microstructure during hot deformation of Al-1Mg-1Mn. *Mater. Sci. Technol.*, 1990, **6**, 453-460.  
doi: 10.1179/mst.1990.6.5.453
15. Roberts, W. & Ahlblom, B. A nucleation criterion for dynamic recrystallization during hot working. *Acta Metallurgica.*, 1978, **26**, 801-813.  
doi:10.1016/0001-6160 (78)90030-5
16. Gottstein, G.; Brünger, E.; Frommert, M.; Goerdeler, M. & Zeng, M. Prediction of the critical conditions for dynamic recrystallization in metals. *Int. J. Mater. Res.*, 2003, **94**, 628-635.  
doi:10.1515/ijmr-2003-0109
17. Shaban, M. & Eghbali, B. Determination of critical conditions for dynamic recrystallization of microalloyed steel. *Mater. Sci. Eng.*, 2010, **527**, 4320–4325.  
doi: 10.1016/j.msea.2010.03.086
18. McQueen, H.J. & Jonas, J.J. Recovery and recrystallization during high temperature deformation. *Treatise on Mater. Sci. Technol.*, 1975, **6**, 393-493.  
doi:10.1016/B978-0-12-341806-7.50014-3
19. Momeni, A., Dehghani, K. & Ebrahimi, G.R. Modeling the initiation of dynamic recrystallization using a dynamic recovery model, *J. Alloys and Compounds*, 2011, **509**, 9387-9393.  
doi: 10.1016/j.jallcom.2011.07.014
20. Wei, Hai-lian; Liu, Guo-quan; Xiao Xiang & Zhang, Ming-he. Dynamic recrystallization behavior of a medium carbon vanadium microalloyed steel. *Mater. Sci. Eng.*, 2013, **573**, 215–221.  
doi: 10.1016/j.msea.2013.03.009
21. Xu, Yaowen; Tang, Di; Song, Yong & Pan, Xiaogang. Dynamic recrystallization kinetics model of X70 pipeline steel. *Mater. Design*, 2012, **39**, 168–174.  
doi: 10.1016/j.matdes.2012.02.034
22. Mirzadeh, H. & Najafizadeh, A. The rate of dynamic recrystallization in 17-4 PH stainless steel. *Mater. Design*, 2010, **31**, 4577–4583.  
doi:10.2355 /isijinternational.53.680
23. Zhao, B.; Zhao, T.; Li, G. & Lu, Q. The kinetics of dynamic recrystallization of a low carbon vanadium-nitride microalloyed steel. *Mater. Sci. Eng. A*, 2014, **604**, 117-121.  
doi:10.1016/j.msea.2014.03.019
24. Kim, Sung-II & Yoo, Yeon-Chul. Dynamic recrystallization behavior of AISI 304 stainless steel. *Mater. Sci. Eng. A*, 2001, **311**, 108-113.  
doi: 10.1016/S0921-5093(01)00917-0
25. Fernández, A.I.; Uranga, P.; López, B. & Rodríguez-Ibabe, J.M. Dynamic recrystallization behavior covering a wide austenite grain size range in Nb and Nb-Ti microalloyed steels. *Mater. Sci. Eng. A*, 2003, **361**, 367–376.  
doi:10.1016/S0921-5093(03)00562-8
26. Charnock, W. & Nutting, J. The effect of carbon and nickel upon the stacking-fault energy of iron. *Mater. Sci. J.*, 1967, **1**, 123-127.  
doi:10.1179/msc.1967.1.1.123
27. Zhao, B.; Li, G.; Yan, P. & Huang, L. Analysis of the methods to calculate austenite static recrystallization volume fraction. *J. Mater. Res.*, 2016, **31**, 2097-2104.  
doi: 10.1557/jmr.2016.217
28. Fernandez, A.I.; Lopez, B. & Rodriguez-Ibabe, J.M. Relationship between the austenite recrystallised fraction and the softening measured from the interrupted torsion test technique. *Scripta Materialia*, 1999, **40**, 543–549.  
doi:10.1016/S1359-6462(98)00452-7
29. Medina, S.F. & Mancilla, J.E. Static recrystallization modelling of hot deformed steels containing several alloying elements. *ISIJ International*, 1996, **36**, 1070-1076.  
doi: 10.2355/isijinternational.36.1070
30. Rollett, A.D.; Srolovitz, D.J.; Doherty, R.D. & Anderson, M.P. Computer simulation of recrystallization in non-uniformly deformed metals. *Acta Metall.*, 1989, **37**, 627-639.  
doi:10.1016/0001-6160 (89)90247-2
31. Mandal, Gopi K.; Das, Siddhartha S.; Kumar, Tipu; Kamaraj, Ashok; Mondal, K. & Srivastava, V.C. Role of precipitates in recrystallization mechanisms of nb-mo

- microalloyed steel. *J. Mater. Eng. Perform.*, 2018, **27**, 6748-6757.  
doi: 10.1007/s11665-018-3711-1
32. Xu, Y.B.; Yu, Y.M.; Xiao, B.L.; Liu, Z.Y. & Wang, G.D. Modelling of microstructure evolution during hot rolling of a high-Nb HSLA steel. *J. Mater. Sci.*, 2010, **45**, 2580–2590.  
doi: 10.1007/s10853-010-4229-6
33. Chatterjee, S.; Verma, A.K. & Mukhopadhyay, A. Static recrystallisation kinetics of austenite in Ti, Nb and V microalloyed steels during hot deformation. *Ironmaking and Steelmaking*, 2007, **34**, 145-150.  
doi: 10.1179/174328107X155231
34. Hodgson, P.D. & Gibbs, R.K. A mathematical model to predict the mechanical properties of hot rolled C-Mn and microalloyed steels. *ISIJ International*, 1992, **32**, 1329-1338.  
doi: 10.2355/isijinternational.32.1329
35. Homsher-Ritosa, Caryn Nicole. Determination of the non-recrystallization temperature ( $T_{NR}$ ) in multiple microalloyed steels. 2001, M. Tech. Thesis, Colorado School of Mines, Golden Colorado.
36. Homsher, C.N. & Van Tyne, C.J. Comparison of two physical simulation tests to determine the non-recrystallization temperature in hot rolled steel plates, 2015.  
doi: 10.1520/MPC20150002
37. Fadel, A.H. & Radovic, N. Determination of activation energy for static recrystallisation in Nb-Ti low carbon microalloyed steel. *Int. J. Eng. Inf. Technol. (IJEIT)*, 2017, **3**, 164-169.
38. Kliber, J.; Fabík, R.; Vitez, I. & Drozd, K. Hot forming recrystallization kinetics in steel. *Metallurgija*, 2010, **49**, 67-71.
39. Capdevila, C.; Cock, T. De; García-Mateo, C., Caballero, F.G. & de Andrés, C.G. Influence of second phase particles on recrystallisation of cold-rolled low carbon microalloyed steels during isothermal annealing. *Mater. Sci. Forum*, 2005, **500–501**, 803-810.  
doi: 10.4028/www.scientific.net/MSF.500-501.803
40. Laasraoui, A. & Jonas, J.J. Recrystallization of austenite after deformation at high temperatures and strain rates—Analysis and modeling. *Metall. Transact. A*, 1991, **22**, 151-160.  
doi: 10.1007/BF03350957

## ACKNOWLEDGEMENT

The authors would like to thank Director, Defence Metallurgical Research Laboratory for providing the continuous support and encouragement for carrying out this work. The authors also thank Mr. LambodarSahoo for his assistance in testing samples in Gleeble.

## CONTRIBUTORS

**Dr Atul Kumar**, obtained his Ph.D. in Materials Science and Engineering from Max Planck Institute for Metals Research, Stuttgart. He is working as Scientist in DRDO-DMRL. His research interests include Mechanical behaviour of metals and alloys both in bulk & small-length scale and thermo-mechanical simulation of metals & alloys in Gleeble. His current contributions are involved in planning of experimental work, analysing the experimental data and manuscript preparation.

**Mr T.V.V.S. Prasad** is a graduate in Mechanical engineering. During his M.Tech. in Materials Technology from NIT Warangal. He performed his M.Tech. project work at DMRL. His areas of interest include: Structure-property correlations in the field of metals and alloys.

His contribution in the present study involves: Carrying out thermo-mechanical testing pertaining to static recrystallisation.

**Mr V.V. Karthik** is a graduate in Mechanical engineering. During his M.Tech. in Materials Engineering from NIT Karnataka, Surathkal, he performed his M.Tech. project work at DMRL. His areas of interest include: Structure-property correlations in the field of metals and alloys.

His contribution in the present study involves: Carrying out thermo-mechanical testing pertaining to dynamic recrystallisation.

**Prof Kumkum Banerjee** is serving as Associate Professor at NIT Karnataka. She obtained her PhD from IIT Kharagpur. Her areas of interest include thermo-mechanical processing of metals, joining of metals, corrosion and hydrogen-embrittlement of metals, etc.

Her contributions for the current work are pertaining to planning of experimental work.

**Dr K. Gopinath** obtained his PhD in Materials Engineering from IISc, Bangalore. He is working as Senior Scientist in DRDO-DMRL. His area of interest includes characterisation of monotonic and cyclic deformation behaviour of advanced wrought and cast superalloys.

His contributions are involved in planning of experimental work, analysing the experimental data and manuscript preparation.

**Dr R. Balamuralikrishnan** obtained his PhD from Carnegie Mellon University, Pittsburgh, USA. He is working as Senior Scientist and Associate Director at DRDO-DMRL. His research interests include the physical metallurgy of high performance steels and nickel base superalloys, with a strong emphasis on advanced microstructural characterisation aimed at furthering the understanding of structure-property correlations in these important engineering materials. He is also interested in applying modelling and simulation tools to study materials and processes.

His contributions are involved in planning of experimental work, analysing the experimental data and manuscript preparation.